

Integration of Nanofiltration for the Sustainable Management of Reverse Osmosis Brines

Antía Pérez-González^a, Raquel Ibáñez^a, Pedro Gómez^b, Ana Urriaga^{*a},
Inmaculada Ortiz^a

^aUniv. Cantabria, Dep. Chemical and Biomolecular Engineering, Avda. Los Castros s/n, 39005 Santander, Spain.

^bAPRIA Systems S.L., Polígono Trascueto s/n, Camargo, Cantabria, Spain.

urriaga@unican.es

The aim of this work is to develop an integrated process for the sustainable management of reverse osmosis brines generated in desalination plants. The core of the proposed process is the bipolar membrane electrodialysis (BMED), which has proved to be a technically feasible option for the conversion of RO desalination brines into HCl and NaOH. However, the overall process should also integrate the brine purification treatment. Precipitation with NaOH, using the reactant produced in BMED, would be the most suitable option for hardness removal. On the other hand, the presence of sulphate affects negatively the quality of the hydrochloric acid product and the current efficiency of BMED. Therefore, in this work nanofiltration (NF) has been applied in order to retain sulphate.

This work reports the mathematical model that describes the transport of binary aqueous solutions of chloride and sulphate anions through the NF270 nanofiltration membrane. The relevance and the difficulty of the task lie on the high concentrations of both anions, as it occurs in the RO brines generated in the desalination of brackish water, and the variety of valence charge of the species, monovalent chloride and divalent sulphate, that introduces significant differences in the interaction of both anions with the charged membrane surface.

1. Introduction

Water shortage problems in dry inland regions are increasingly satisfied through reverse osmosis (RO) desalination of brackish groundwater's resources. Exploitation of brackish groundwaters is advantageous due to the lower salt concentration of the inlet water compared to seawater, which reduces the osmotic pressure to be overcome and the energy consumption (Muñoz and Fernández-Alba, 2008). However, the management of concentrates is an important drawback because brine discharges from inland installations still remains being a problem with not many feasible alternatives (Zarzo and Campos, 2011).

Alternatives aiming at zero liquid discharge, through combination of different technologies, are highlighted as the most promising management options (Pérez-González et al., 2012). In this work a sequential process based on the appropriate combination of advanced separation technologies is proposed with the aim of reducing the adverse environmental impact of brine discharge, together with the recovery of valuable products contained in the concentrated brine. The strategy to achieve this goal implies, first, a pretreatment step of the brine to remove scaling salts and impurities. Next Bipolar Membrane Electrodialysis (BMED) is used to recover hydrochloric acid (HCl) and sodium hydroxide (NaOH) from the pre-treated brine. This technology has proved to be technically feasible for the production of 1.0 M or higher acid and base solutions (Ibáñez et al., 2012). Current research is focused on pretreatment stage, specifically in the reduction of sulphate concentration to avoid its negative effects in BMED (Prisciandaro et al., 2013). Therefore, in this work nanofiltration (NF) has been applied in order to retain sulphate compounds.

Nanofiltration is a pressure driven membrane separation process with characteristics between reverse osmosis and ultrafiltration. NF membranes are typically polymeric, asymmetric and consist of a low resistance support layer with a functionally active porous top layer (Oatley et al., 2012). Nanofiltration

membranes have properties that combine size and electrical effects. The pores are typically near 1 nm in diameter and have fixed charges. Due to these characteristics, NF membranes retain multivalent complex ions and transmit small uncharged solutes and low charged ions. This, along with the small energy consumption of the process and the high fluxes attained, makes nanofiltration membranes extremely useful in fractionation and selective removal of solutes from complex process streams (Benavente et al., 2010). Membrane nanofiltration is extremely complex and is dependent on the micro-hydrodynamics and interfacial events occurring at the membrane surface and within the membrane nanopores. There is significant debate as to the exact nature of these complex phenomena and rejection is typically attributed to a combination of steric and electrical effects (Oatley et al., 2012).

The design of the integrated membrane process requires of a reliable mathematical model that enables the prediction of the nanofiltration stage under variable conditions of brine composition and operating pressure. Experimental data were obtained using feed solutions with a sulphate content of 0.1 M and chloride concentrations in the range 0.2 -1.2 M, to include the concentration levels found in brines generated in brackish water desalination and seawater desalination.

2. Theoretical background

The presented model is based on the Donnan steric pore model and dielectric exclusion (DSPM&DE) presented by Bandini and Vezzani (2003). This model is basically an extension of the Donnan steric pore model (DSPM) firstly proposed by Bowen and Mukhtar (1996), and then revised in Bowen et al. (1997) and in Bowen and Mohammad (1998). The transport equations of ions through the membrane are based on the extended Nernst–Planck equation, accounting for ionic diffusion, electromigration and convection in the membrane pores; the hindered nature of diffusion and convection of the species inside the membrane is considered. Ionic partitioning at the interfaces between the membrane and the external liquid phases takes into account of three separation mechanisms: steric hindrance, Donnan equilibrium and dielectric exclusion.

The modelling of mass transport in nanofiltration accounts for: (a) equilibrium partitioning of species at the feed/membrane interface; (b) solute transport through the pores by a combination of convection, diffusion and electromigration; (c) equilibrium partitioning of species at the membrane/permeate interface. Basic equations of the model are reported in Table 1.

The membrane is characterized through three parameters which allow achieving the permeate concentrations with the NF model: membrane pore radius (r_p), effective membrane thickness (δ) and effective membrane charge density (X_d). The membrane charge originates from the dissociation of ionisable groups at the membrane surface and from the inner membrane pore structure. The magnitude of the “effective membrane charge density” is usually determined as a fitting parameter dependant on the concentration of ionic solutions. Currently there is no direct measurement technique available for this parameter or any fundamental description suitable to directly relate the parameter to an alternative measured value, i.e, membrane zeta potential or similar (Oatley et al., 2012).

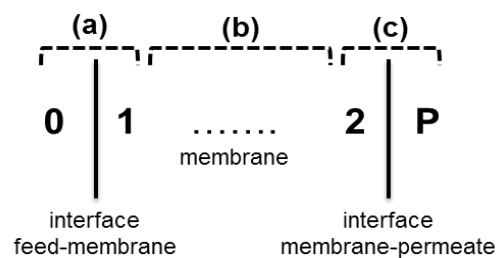


Figure 1: Profiles and interfaces along the membrane

3. Experimental materials and methods

The salinity of brackish groundwaters water ranges from 1,000 to 8,000 mg/L of total dissolved solids (TDS) while the value for marine water is typically 35,000 mg/L TDS (Martinetti et al., 2009). However, constituent concentrations in the RO brines are found to be double or higher than in feed water.

Table 1: Basic equations of the proposed NF model. Reference is made to the coordinate system reported in Figure 1

		Notation
(a) Partitioning at the feed-membrane interface		c concentration (mol m ⁻³)
$\frac{c1_i}{c0_i} = \phi_i \exp[-z_i \Delta\psi_{Donnan}(0)] \exp(-\Delta W_i)$	(1)	D_p hindered diffusivity (m ² s ⁻¹)
(b) Transport of ions through the membrane		D_∞ diffusivity of ions (m ² s ⁻¹)
$j_i = J_v K_{c_i} \bar{c}_i - D_{p_i} \frac{c1_i - c2_i}{\delta} - z_i \bar{c}_i D_{p_i} \frac{F}{R_{gas} T} \frac{\Delta\phi}{\delta}$	(2)	e electronic charge (C)
$\frac{\Delta\phi}{\delta} = \frac{\sum_{i=1}^n z_i \frac{J_v}{D_{p_i}} [K_{c_i} \bar{c}_i - cP_i]}{\frac{F}{R_{gas} T} \sum_{i=1}^n z_i^2 \bar{c}_i}$	(3)	F Faraday constant (C/mol)
$\bar{c}_i = \frac{c1_i + c2_i}{2}$	(4)	j molar solute flux (mol m ⁻² s ⁻¹)
$j_i = J_v \cdot cP_i$	(5)	J_V total volume flux (m s ⁻¹)
$D_{p_i} = K_{d_i} \cdot D_{\infty_i}$	(6)	K_c convective hindrance factor, dimensionless
Hindrance factors		K_d diffusive hindrance factor, dimensionless
$K_{d_i} = 1.0 - 2.30\lambda_i + 1.154\lambda_i^2 + 0.224\lambda_i^3$	(7)	r_i Stoke radius of ion (m)
$K_{c_i} = 1.0 + 0.054\lambda_i - 0.988\lambda_i^2 + 0.441\lambda_i^3$	(8)	r_p effective membrane pore radius (m)
(c) Partitioning at the membrane-permeate interface		R_{gas} universal constant of gases (J mol ⁻¹ K ⁻¹)
$\frac{c2_i}{cP_i} = \phi_i \exp[-z_i \Delta\psi_{Donnan}(\delta)] \exp(-\Delta W_i)$	(9)	T absolute temperature (K)
Steric partitioning		X_d effective membrane charge density (mol m ⁻³)
$\phi_i = (1 - \lambda_i)^2$	(10)	z ionic valence, dimensionless
$\lambda_i = \frac{r_i}{r_p}$	(11)	α hydration radius (m)
Dielectric exclusion		δ effective membrane thickness (m)
$\Delta W_i = \frac{z_i^2 e^2}{8\pi\epsilon_0\alpha_i} \left(\frac{1}{\epsilon_p} - \frac{1}{\epsilon_b} \right)$	(12)	$\Delta\psi_{Donnan}$ Donnan potential, dimensionless
$\epsilon_p = \frac{5}{8} \epsilon_b$	(13)	ΔW Dielectric exclusion, dimensionless
Electroneutrality conditions		ϵ_0 vacuum permittivity (C/m V)
$\sum_{i=1}^n z_i cP_i = 0$	(14)	ϵ_b dielectric constant of the bulk solution (C ² /J m)
$\sum_{i=1}^n z_i c1_i + X_d = 0$	(15)	ϵ_p : dielectric constant of the pore solution (C ² /J m)
$\sum_{i=1}^n z_i c2_i + X_d = 0$	(16)	Subscripts
		i ion

Table 2, shows the chemical characterization of real RO brines obtained from one brackish water desalination plant (Cuevas de Almanzora) and from two seawater desalination plants (Carboneras and Las Aguilas) located in Spain; additionally, the characteristics of brackish water desalination brines (Martinetti et al., 2009) and seawater desalination brines (Ji et al., 2010) given in the literature are included for comparison purposes. Taking into account these characterizations, it can be seen that RO brines could become an important salts resource, and valuable compounds can be recovered by applying an adequate treatment. The presence of sulphate is an important inconvenient. Particularly, in referenced RO brines from Spanish desalination plants, sulphate is quite abundant as a consequence of the geological characteristics of the area, rich in gypsum. Sulphate migration through anionic exchange membranes towards the acid stack is one of the factors affecting the current efficiency of BMED (Ibáñez et al., 2012). Therefore, in this work nanofiltration (NF) has been applied in order to retain sulphate compounds (Bargeman et al., 2009). According to the literature (Hilal et al. 2007), membrane NF270 (Dow FilmTec) has been selected. The feed compositions and the operating parameters play a major role for the separation performance of NF membranes (Wessely and Samhaber, 2013). Therefore, synthetic solutions with a sulphate content of 0.1 M and chloride concentrations in the range 0.2 -1.2 M were employed, to include the concentration levels of brines generated in brackish water desalination and seawater desalination.

Table 2: Chemical characterization of the RO brines referenced in this work (Cuevas de Almazora, Carboneras, Las Aguilas). Values are compared with literature data

Parameter	Brackish water desalination brines		Seawater desalination brines		
	Cuevas de Almazora ⁽¹⁾	Martinetti et al., 2009	Carboneras ⁽¹⁾	Las Aguilas ⁽¹⁾	Ji et al., 2010
pH	7.9	8	8	9	8.2
Conductivity(μS/cm)	34,300	-	95,500	-	-
TDS (mg/L)	20,700	17,500	70,000	70,488	50,200
Chloride (mg/L)	7,279	8,960	37,240	38,887	28,800
Sulphate (mg/L)	8,465	1,920	7,243	5,316	3,060
Sodium (mg/L)	5,176	5,130	17,020	21,922	15,500
Magnesium (mg/L)	1,589	386	2,715	2,479	2,020
Calcium (mg/L)	1,828	819			
Carbonate (mg/L)	0	-	18	155	199
Bicarbonate (mg/L)	826	223	217	173	-

⁽¹⁾ Real concentrates from desalination plants located in Spain.

All membrane experiments were carried out in a laboratory-scale test cell using a SEPA-CF (GEOsmonics, France) cross-flow module. The membrane area was 0.014 m² and total recirculation was used for both the permeate and the concentrate streams that were returned to the feed reservoir. The feed was pressurized at three pressure values of 5, 10 and 20 bar, with a cross flow rate value (tangential recirculation of the feed stream) of 2.5 L/min. The permeate chamber was maintained at atmospheric pressure. The solute concentration in the feed, permeate and concentrate samples was determined by ion chromatography (Dionex ICS-1100, Sunnyvale, CA, USA) provided with an AS9-HC column for the determination of anions and with a CS12A column for the determination of cations.

The NF270 membrane is a thin film composite of polyester support matrix, microporous polysulfone interlayer and polyamide barrier layer. A mass transfer study in the same cell (SEPA-CF) and the same membrane (NF270) showed low concentration polarization, even for high transmembrane flux conditions (Oatley et al., 2012). Therefore, polarization effects have not been taken into account in this study. The model has been solved using Aspen Custom Modeller (AspenTech), and the unknown parameters related to the morphology and surface charge of the membrane, have been estimated by comparison of the model simulations with the experimental results of hydraulic flux, and chloride and sulphate rejections.

4. Results and discussion

Experiments were performed in triplicate (average standard deviation amongst replicas 0.6 %) and the results of salt rejection versus volume flux are shown in Figure 2. Sulphate rejection was in the range 75-96 % while chloride rejections were between -2 and 17 %. As can be observed from the results, increasing the salt concentration reduced the retention ability of the membranes due to the decrease in Donnan effect (Jiraratananon et al., 2000). This is the reason that explains the reduction in sulphate rejection at increasing chloride concentration.

To simulate the experimental results is necessary to determine the membrane parameters. The value of membrane pore radius of the NF270 membrane was taken from Lin et al.(2007) and Oatley et al. (2012), being $r_p=0.43$ nm. The thickness of the effective NF layer of the membrane was determined through SEM microscopy, being $\delta=7$ μm.

According to the literature (Bowen and Mukhtar, 1996), the dependence between the effective membrane charge density and the bulk ionic concentration lies on a single Freundlich type isotherm. In this work, X_d was estimated from the experimental data of rejection vs. volume flux, thus a value of X_d was estimated for each feed concentration. The obtained values fit according to the equation $X_d=-0.04 \cdot C_{eq}^{1.32}$, being C_{eq} the equivalent concentration of ions in the feed solution, expressed in mol m⁻³. The simulated results obtained are showed in Figure 2.

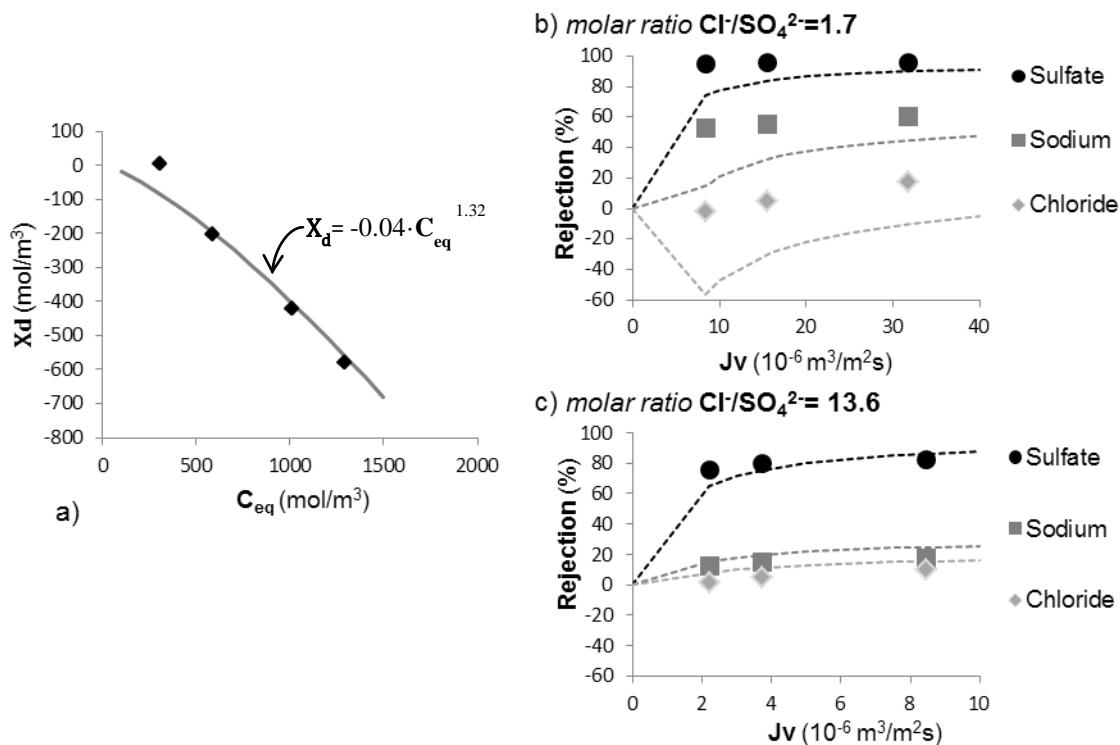


Figure 2: a) Freundlich type isotherm: X_d as function of C_{eq} . Estimated X_d values (\blacklozenge); b) and c) Experimental (solid symbols) and predicted (dashed lines) rejections of NF270 membrane in mixtures of NaCl and Na₂SO₄ solutions at molar ratios of 1.7 and 13.6

Simulation of rejections achieved with the NF model proposed is quite good although deviation of predicted rejections for the lowest molar ratio ($Cl^-/SO_4^{2-} = 1.7$) is high enough, particularly for the rejection of chloride. The magnitude of the effective membrane charge density calculated is physically unrealistic for this molar ratio, as can be seen in Figure 2.a), causing higher deviation between experimental and predicted rejections. Nevertheless, a comparison between simulated and experimental values was made in order to quantify these appreciations. The standard deviation value for rejection description was calculated as 5 % for sulphate, 7 % for sodium and 11 % for chloride. Regarding to the accuracy of simulated results, a parity analysis was done. 83 % of the simulated results fall within the interval $R_{exp} \pm 10 \% R_{exp}$ for sulphate rejection. The parity analysis regarding chloride indicates that the results achieved with the proposed model do not fit in an adequate way with experimental results, which can be related with the estimation of effective membrane charge density and the relation of this parameter with bulk concentration.

5. Conclusions

This work propose a version of the Donnan steric pore model and dielectric exclusion model (DSPM&DE) to describe the rejection of ions in nanofiltration (NF) operations applied to multicomponent salt mixtures that represent the brines from reverse osmosis desalination processes. The model satisfactorily describes the behavior of the rejection of species (chloride, sulphate and sodium) with a good precision, especially for sulphate rejection: the standard deviation between simulated and experimental results was 5 %, and the parity analysis showed that 83 % of simulated rejection values fell within $R_{exp} \pm 10 \% R_{exp}$.

Usually, the NF membrane is characterized through the use of adjustable parameters. The innovative aspect of this study is the use of fixed values for the average pore radius and the effective membrane thickness, based on literature and membrane analysis methods (SEM images). However, the experimental measurement of the effective membrane charge was not attained due to the high concentrations of the brines. In the present study, the effective membrane charge was determined using parametric estimation by comparison of the model predictions with the experimental results. Further studies will be developed in order to determine the effective membrane charge with the objective of achieving a completely predictive nanofiltration model.

Acknowledgements

This work has been financially supported by projects CTQ2008-0690, ENE2010-15585 and CTM2011-23912 (co-financed by ERDF Funds). The authors would like to acknowledge SADYT, S.A. for providing assistance for this work.

References

- Bandini S., Vezzani D., 2003, Nanofiltration modeling: the role of dielectric exclusion in membrane characterization, *Chem. Eng. Sci.*, 58, 3303-3326.
- Bargeman G., Steensma M., ten Kate A., Westerink J.B., Demmer R.L.M., Bakkenes H., Manuhutu C.F.H., 2009, Nanofiltration as energy-efficient solution for sulfate waste in vacuum salt production, *Desalination*, 245, 460-468.
- Benavente J., Silva V., Prádanos P., Palacio L., Hernández A., Jonson G., 2010, Comparison of the volume charge density of nanofiltration membranes obtained from retention and conductivity experiments, *Langmuir*, 26(14), 11841-11849.
- Bowen W.R., Mohammad A.W., 1998, Diafiltration by Nanofiltration: Prediction and Optimization, *AIChE Journal*, 44, 1799-1812.
- Bowen W.R., Mohammad A.W., Hilal N., 1997, Characterisation of nanofiltration membranes for predictive purposes-use of salts, uncharged solutes and atomic force microscopy, *J. Memb. Sci.*, 126, 91-105.
- Bowen W.R., Mukhtar H., 1996, Characterisation and prediction of separation performance of nanofiltration membranes, *J. Memb. Sci.*, 112, 263-274.
- Hilal N., Al-Zoubi H., Mohammad A.W., Darwish N.A., 2007, Performance of nanofiltration membranes in the treatment of synthetic and real seawater, *Sep. Sci. and Tech.*, 42, 493-515.
- Ibáñez R., Pérez-González A., Gómez P., Urtiaga A.M., Ortiz I., 2013, Acid and base recovery from softened reverse osmosis (RO) brines. Experimental assessment using model concentrates. *Desalination*, 309, 165-170.
- Ji X., Curcio E., Al Obaidani S., Di Profio G., Fontananova E., Drioli E., 2010, Membrane distillation-crystallization of seawater reverse osmosis brines, *Sep. Purif. Technol.*, 71(1), 76-82.
- Jiratananon R., Sungpet A., Luangsovan P., 2000, Performance evaluation of nanofiltration membranes for treatment of effluents containing reactive dye and salt, *Desalination*, 130, 177-183.
- Lin Y.L., Chiang P.C., Chang E.E., 2007, Removal of small trihalomethane precursors from aqueous solution by nanofiltration, *J. Hazard. Mater.*, 146, 20-29.
- Martinetti C.R., Childress A.E., Cath T.Y., 2009, High recovery of concentrated RO brines using forward osmosis and membrane distillation, *J. Memb. Sci.*, 331, 31-39.
- Muñoz I., Fernández-Alba A.R., 2008, Reducing the environmental impacts of reverse osmosis desalination by using brackish groundwater resources, *Water Res.*, 42(3), 801-811.
- Oatley D.L., Llenas L., Pérez R., Williams P.M., Martínez-Lladó X., Rovira M., 2012, Review of the dielectric properties of nanofiltration membranes and verification of the single oriented layer approximation, *Adv. Colloid Interface Sci.*, 173, 1-11.
- Pérez-González A., Urtiaga A.M., Ibáñez R., Ortiz I., 2012, State of the art and review on the treatment technologies of water reverse osmosis concentrates, *Water Res.*, 46(2), 267-283.
- Prisciandaro M., Lancia A., Mazzioni Di Celso G., Musmarra D., 2013, Antiscalants for gypsum precipitation in industrial equipments: comparison among different additives, *Chemical Engineering Transactions*, 32, 2137-2142 DOI: 10.3303/CET1332357.
- Wessely L., Samhaber W.M., 2013, Separation performance of polymer membranes for organic solvent mixtures, *Chemical Engineering Transactions*, 32, 1885-1890 DOI: 10.3301/CET1332315.
- Zarzo D., Campos E., 2011, Project for the development of innovative solutions for brines from desalination plants, *Deswater*, 31, 206-217.